Theoretical interpretation of a pronounced permeability scale effect in unsaturated fractured tuff

Yunjung Hyun,[1] Shlomo P. Neuman,[1] Velimir V. Vesselinov,[2] Walter A. Illman,[3] Daniel M. Tartakovsky,[2] and Vittorio Di Federico[4]

Received 10 May 2001; revised 8 January 2002; accepted 8 January 2002; published 27 June 2002.

[1] Numerous single-hole and cross-hole pneumatic injection tests have been conducted in unsaturated fractured tuff at the Apache Leap Research Site (ALRS) near Superior, Arizona. Single-hole tests have yielded values of air permeability at various locations throughout the tested rock volume on a nominal scale of ~1 m. Cross-hole tests have yielded equivalent air permeabilities (and air-filled porosities) for a rock volume characterized by a length scale of several tens of meters. Cross-hole tests have also provided high-resolution tomographic estimates of how air permeability (and air-filled porosity), defined over grid blocks having a length scale of 1 m, vary throughout a similar rock volume. The results have revealed a highly pronounced scale effect in permeability (and porosity) at the ALRS. We examine the extent to which the permeability scale effect is amenable to interpretation by a recent stochastic scaling theory, which treats the rock as a truncated random fractal. *INDEX TERMS:* 1869 Hydrology: Stochastic Processes; 1875 Hydrology: Unsaturated Zone; 3260 Mathematical Geophysics: Inverse Theory; 3250 Mathematical Geophysics: Fractals and Multifractals; *KEYWORDS:* scaling, permeability, fractals, fractured rocks

1. Multiscale Pneumatic Tests at the Apache Leap Research Site

[2] Numerous single-hole [*Guzman et al.*, 1994, 1996] and cross-hole [*Illman et al.*, 1998] pneumatic injection tests have been conducted by our group at the Apache Leap Research Site (ALRS) near Superior, Arizona. The site included 22 vertical and inclined (at 45°) boreholes completed to a maximum vertical depth of 30 m within a layer of slightly welded unsaturated tuff. Of >270 single-hole tests, 184 were conducted in boreholes V2, W2a, X2, Y2, Y3, and Z2 by setting the packers 1 m apart (as illustrated by dark circles in Figure 1). Cross-hole tests were conducted in 16 boreholes belonging to sets V, W, X, Y, and Z as illustrated in Figure 2. Among numerous phenomenological results revealed by these tests [*Chen et al.*, 2000], the following two are most directly relevant to this paper: (1) the pneumatic pressure behavior of fractured tuff at the site is amenable to analysis by treating the rock as a single (as opposed to dual) continuum on scales ranging from meters to tens of meters, and (2) this continuum is representative primarily of interconnected fractures (rock matrix having little effect on the observed pneumatic behavior). Both the single-hole and cross-hole test results have proven to be virtually free of skin effect [*Illman and Neuman*, 2000, 2001], implying that they represent rock conditions unperturbed by the presence of boreholes.

1.1. Single-Hole Pneumatic Injection Tests

[3] Air permeability data obtained from a steady state interpretation of the 184 single-hole tests in 1-m borehole intervals were first analyzed geostatistically by Guzman and Neuman (discussed in the work of *Rasmussen et al.* [1996]). The authors found directional sample (semi)variograms of $\log_{10}k$ to be noisy and difficult to interpret. *Chen et al.* [2000] found it possible to eliminate directional effects from the variogram by accounting for spatial drift in the data. They, however, concluded that an equally good representation of the data is obtained by fitting a power model $\gamma(s) = C_0 s^{2H}$ to the omnidirectional sample variogram in Figure 3, where s is distance (lag), C_0 is a constant, and H is the Hurst coefficient.

[4] Considering that models with drift entail many more parameters than the power model, *Chen et al.* [2000] selected the latter to obtain a kriged estimate of how log permeability varies in three-dimensional space. Their estimate is based on an augmented database of 227 $\log_{10}k$ values, including 43 values obtained earlier by *Rasmussen et al.* [1990, 1993]. The latter values derive from a steady state interpretation of single-hole tests in 3 m intervals within boreholes X1, X3, Y1, Z1, and Z3, which have not been tested by *Guzman et al.* [1994, 1996]. Statistics of the original and augmented data and of the kriging results are summarized in Table 1.

1.2. Cross-Hole Pneumatic Injection Tests

[5] *Illman and Neuman* [2001] used type curves to interpret the results of a cross-hole test, labeled PP4, by treating the fractured rock as a uniform isotropic continuum. Their analysis yielded a set of equivalent directional air permeability (and air-filled porosity) estimates for each pair of borehole injection and monitoring intervals. The corresponding $\log_{10}k$ estimates are summarized statistically in Table 1.

[6] *Vesselinov et al.* [2001a, 2001b] used a three-dimensional numerical inverse model to interpret several cross-

[1]Department of Hydrology and Water Resources, University of Arizona, Tucson, Arizona, 85721.
[2]Los Alamos National Laboratory, Los Alamos, New Mexico 87545.
[3]University of Iowa, Iowa City, IA 52242.
[4]University of Bologna, Bologna, Italy.

0043-1397/02/2001WR000658$09.00

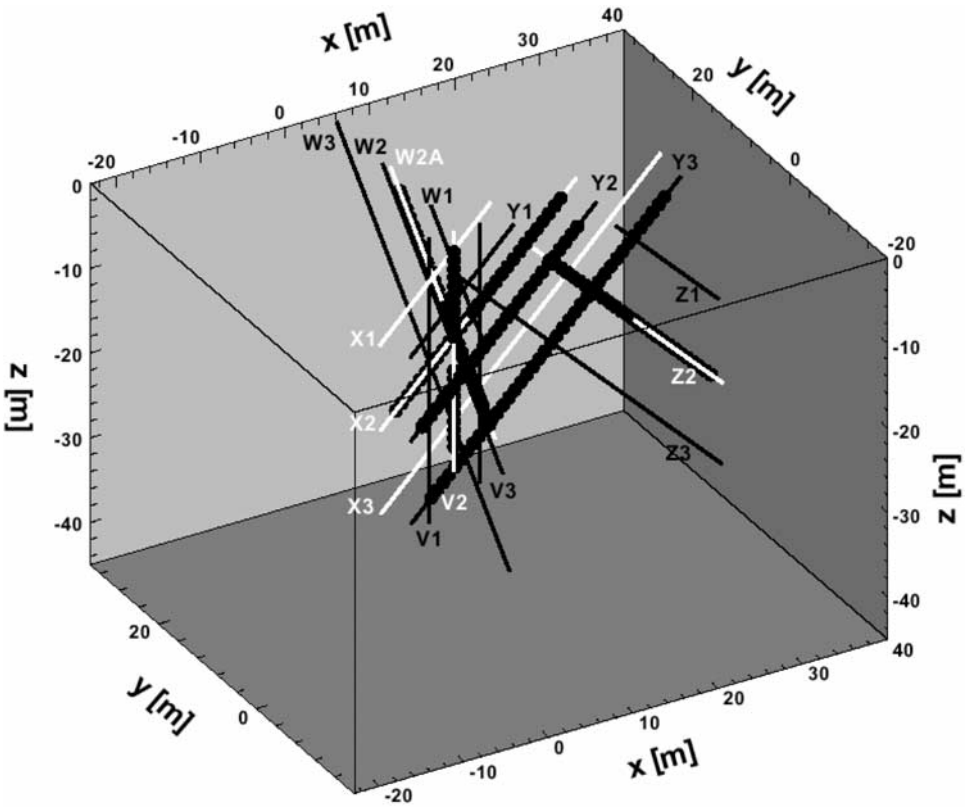

Figure 1. Center locations (solid circles) of 1-m single-hole pneumatic test intervals; overlapping circles indicate retested locations [after *Illman and Neuman*, 2001].

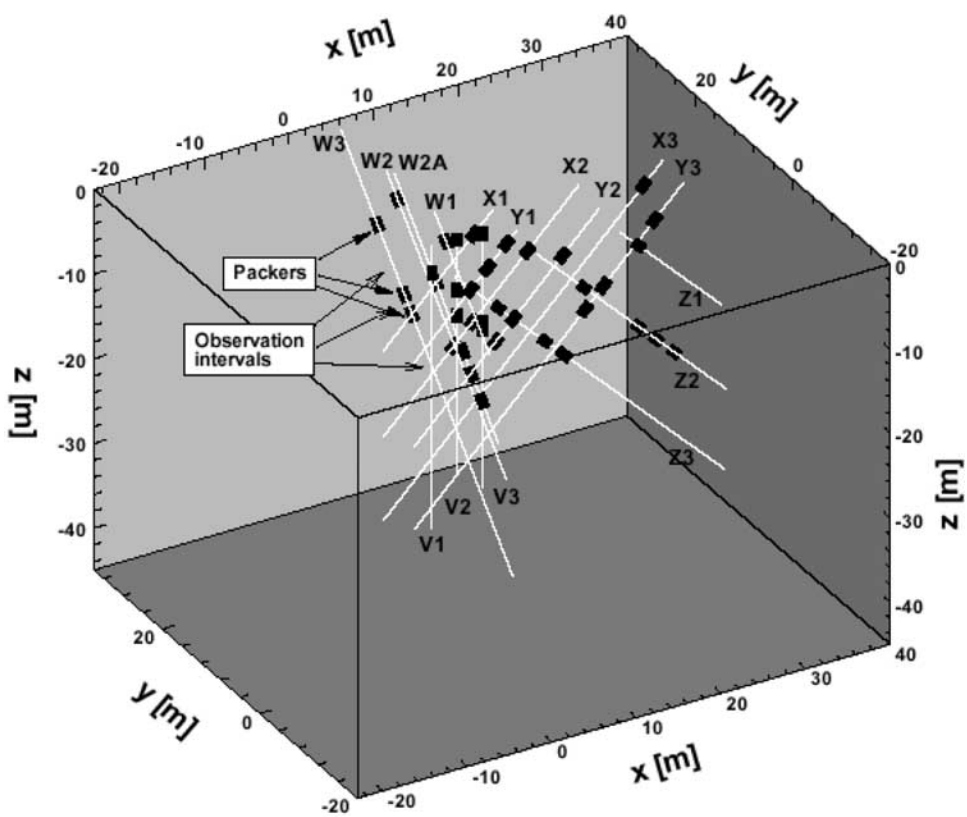

Figure 2. Locations of packers during cross-hole tests PP4-7 [after *Vesselinov et al.*, 2001a].

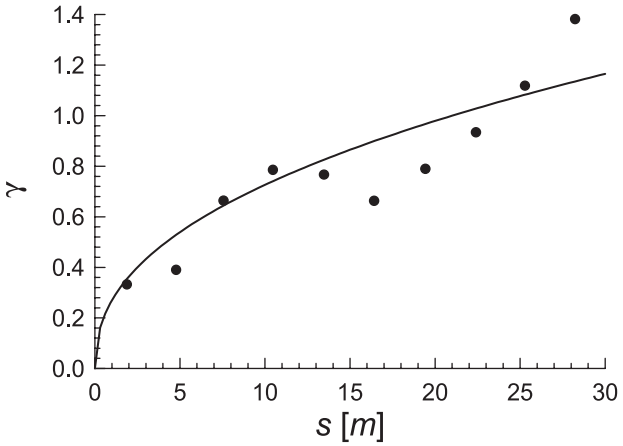

Figure 3. Omnidirectional sample variogram and power model of 1-m scale single-hole $\log_{10}k$ data.

hole pneumatic tests at the ALRS. They analyzed pneumatic cross-hole test data by treating the rock as being either (1) spatially uniform or (2) a random fractal characterized by a power variogram. The first approach yielded a series of equivalent log air permeability (and log air-filled porosity) estimates analogous to the type curve estimates of *Illman and Neuman* [2001]. The second approach yielded a high-resolution estimate of how air permeability and air-filled porosity, defined on grid blocks having a length scale of 1 m, vary spatially throughout the tested rock volume. The approach entailed geostatistical inversion of the cross-hole test data to yield estimates at "pilot points." Projecting these estimates onto the simulation domain by kriging yields a "tomographic" image of rock heterogeneity. Results obtained by the authors for tests labeled PP4-PP6, using both approaches, are summarized statistically in Table 1.

1.3. Permeability Scale Effect

[7] Table 1 reveals a steep increase in the mean value of $\log_{10}k$ estimates with the scales of observation and/or resolution. The smallest scale, on the order of 1 m, corresponds to single-hole test results and to tomographic (kriged) inverse estimates based on the cross-hole tests. The largest scale, on the order of tens of meters, corresponds to type curve results and to inverse estimates of equivalent log permeability obtained from cross-hole tests upon treating the rock as being uniform. Mean values obtained by different methods at any given scale of estimation are generally comparable. Yet mean values obtained from cross-hole tests under the uniform rock assumption are consistently larger than those obtained by allowing pneumatic properties to vary spatially over distances of 1 m.

[8] For example, the mean of inverse $\log_{10}k$ estimates obtained from tests PP4, PP5, and PP6 when treating the rock as being spatially uniform (−13.70) exceeds the mean of simultaneous tomographic estimates from the same three tests (−15.69) by 1.99. This represents a 98-fold increase in the associated values of k. The mean of $\log_{10}k$ estimates obtained by inverting cross-hole test PP4 when treating the rock as being uniform (−13.57) exceeds the average of mean tomographic estimates obtained from this test using 64 pilot points (−14.77) by 1.20. This represents an increase in the associated values of k by a factor of ∼16. The average of all uniform inverse mean estimates in Table 1 (−13.64) exceeds that of all tomographic mean estimates (−15.23) by 1.59, which corresponds to an increase in the associated value of k by a factor of 39. It is thus clear that estimates of air permeability increase markedly with scale at the ALRS. On the other hand, the variances of inverse $\log_{10}k$ estimates is seen in Table 1 to decrease with scale, as one should anticipate.

[9] This permeability scale effect is clearly unrelated to the method of testing: there is consistency between single-hole and cross-hole test results corresponding to a wide range of injection rates and to steady state as well as transient flow regimes. The scale effect is likewise unrelated to the method of test interpretation: there is consistency between results obtained by means of steady state analytical formulae from single-hole test data [*Guzman et al.*, 1996], which are shown elsewhere to compare well with transient type curve [*Illman and Neuman*, 2000] and inverse [*Vesselinov and Neuman*, 2001] analyses of the same data, and type curve [*Illman and Neuman*, 2001] as

Table 1. Summary Statistics of $\text{Log}_{10}k$ Estimated in Various Ways[a]

Source	Data Estimates				Kriging Estimates			
	Sample Size	Mean	Variance	CV	Sample Size	Mean	Variance	CV
Single-hole tests (1 m)	184	−15.25	0.76	−0.050				
Single-hole tests (1 m + 3 m)	227	−15.22	0.87	−0.061	53176	−15.20	0.45	−0.044
Cross-hole tests (type curve analysis)		−13.49	0.33	−0.043				
Uniform (equivalent) estimates								
PP4	30	−13.46	0.34	−0.043	–	–	–	–
Cross-hole tests (numerical inversion)								
Uniform (equivalent) estimates								
PP4	32	−13.57	0.57	−0.056	–	–	–	–
PP4–PP6	76	−13.70	0.43	−0.048	–	–	–	–
Nonuniform (tomographic) estimates								
PP4: 32 pilot points	–	–	–	–	53176	−15.23	1.67	−0.085
PP4: 64 pilot points	–	–	–	–	53176	−14.77	1.62	−0.086
PP4–PP6: 72 pilot points	–	–	–	–	53176	−15.69	1.93	−0.089

[a] $\text{Log}_{10}k$ values are m^2. CV is coefficient of variance.

well as numerical inverse [*Vesselinov et al.*, 2001a, 2001b] interpretations of cross-hole test data. Contrary to a recent suggestion in the literature [*Butler and Healey*, 1998a, 1998b], the observed scaling behavior is not an artifact of rock conditions around the injection borehole: neither the single-hole [*Illman and Neuman*, 2000] nor the cross-hole [*Illman and Neuman*, 2001] test results have been affected by any skin effect of consequence. The pronounced permeability scale effect we have observed at the ALRS appears to be real.

1.4. Previous Observations and Explanations of Permeability Scale Effect

[10] Variations of permeability or transmissivity with scale have been observed previously in a variety of hydrogeologic settings [*Bradbury and Muldoon*, 1990; *Rovey and Cherkauer*, 1995; *Tidwell and Wilson*, 1997; *Sánchez-Villa et al.*, 1996; *Schulze-Makuch et al.*, 1999]. According to *Geldon* [1996], cross-hole tests conducted in saturated fractured tuffs and lavas of the Calico Hills and Crater Flat Tuff formations at Yucca Mountain, Nevada, have yielded transmissivities and hydraulic conductivities that are $\sim$2 orders of magnitude larger than those obtained from single-hole tests. A scale effect of similar magnitude was noted by *Martínez-Landa et al.* [2000] when comparing the results of pulse, Horner, cross-hole, and inflow tests in a saturated block of fractured granite at the Grimsel underground laboratory in Switzerland.

[11] Some authors have dismissed these scale effects as artifacts of a skin effect due to inadequate development of borehole test intervals [*Butler and Healey*, 1998a, 1998b]. We have already mentioned that this does not apply to the ALRS. *Rovey and Niemann* [2001] have demonstrated that skin effect was at most of minor importance in their analysis of hydraulic test data from an outwash sand.

[12] *Rovey* [1998] has shown numerically that a scale effect may arise from the dual nature of a porous fractured rock. We have already mentioned that this does not apply to pneumatic tests at the ALRS in which airflow was restricted largely to fractures, the matrix having remained almost completely saturated with water.

[13] *Sánchez-Villa et al.* [1996] have demonstrated numerically that randomly varying transmissivities could exhibit a scale effect due to deviations from log normal distribution. At the ALRS, spatial increments of 1-m scale $\log_{10}k$ data corresponding to lags of 1–3 m are indeed represented more accurately by a Lévy stable than by a Gaussian distribution (Y. Hyun, Analysis of permeability scaling in porous and fractured media, University of Arizona, Tucson, Ph.D. thesis, in preparation, 2002). However, increments corresponding to lags of 6–25 m are virtually Gaussian. In fact, fitting the 1-m scale data to a universal multifractal model [*Schertzer and Lovejoy*, 1989; *Schmitt et al.*, 1995] has yielded $\alpha = 1.86$, which is only slightly below the Gaussian value of 2.

[14] According to *Neuman* [1994], one may be able to explain observed scale variations in the apparent spatial correlation scale and magnitude of log permeability and transmissivity at various sites by treating $\log_{10}k$ as a multivariate Gaussian random field with homogeneous spatial increments, characterized by a power variogram. Such a field is equivalent to fractional Brownian motion (FBM), which has a unique fractal dimension. We have seen that 1-m scale $\log_{10}k$ data from the ALRS can indeed be represented by a power variogram. Though the same data can also be represented by a multifractal model, the latter has a relatively small fractal codimension, $C_{UM} = 0.07$ (Hyun, in preparation, 2002). It thus appears that the 1-m scale $\log_{10}k$ data from the ALRS can be treated without much loss of accuracy as belonging to an FBM.

[15] *Neuman*'s [1994] interpretation of the permeability scale effect accounted indirectly for the effect of domain boundaries. A direct way to do so was found more recently by *Di Federico et al.* [1999]. The purpose of this paper is to examine the degree to which their theory is compatible with the observed permeability scale effect at the ALRS.

2. Theoretical Background

[16] We recount briefly some key theoretical results by *Di Federico and Neuman* [1997] and *Di Federico et al.* [1999], which are required for our analysis. Di Federico et al. have accounted for statistical anisotropy. However, we mentioned earlier that the ALRS data do not lend themselves to representation by a classical anisotropic variogram model. We therefore limit our theoretical discussion to the statistically isotropic case.

2.1. Random Fields With Truncated Power Variograms

[17] Consider a statistically isotropic random field with homogeneous spatial increments, characterized by a power variogram. According to *Di Federico and Neuman* [1997], such a field can be viewed as consisting of an infinite hierarchy of homogeneous, mutually uncorrelated fields or modes having either exponential or Gaussian variograms. Upon introducing lower and upper cutoffs, $n_l = 1/\lambda_l$ and, $n_u = 1/\lambda_u$ all modes with integral scales $\lambda > \lambda_l$ and $\lambda < \lambda_u$ are filtered out (excluded). The integral scales of the lowest- and highest-frequency cutoff modes are related to the length scales of the sampling window (domain) and data support (sample volume), respectively. The resultant field has a variogram

$$\gamma(s^*, n_l, n_u) = \gamma(s^*, n_l) - \gamma(s^*, n_u), \tag{1}$$

where, for exponential modes ($0 < H < 1/2$),

$$\gamma(s, n_m) = \frac{C}{2Hn_m^{2H}}\left[1 - \exp(-n_m s) \quad + (n_m s)^{2H}\Gamma(1-2H, n_m s)\right] \tag{2}$$

and, for Gaussian modes ($0 < H < 1$),

$$\gamma(s, n_m) = \frac{C}{2Hn_m^{2H}}\left[1 - \exp\left(-\frac{\pi}{4}n_m^2 s^2\right) + \left(\frac{\pi}{4}n_m^2 s^2\right)^H \Gamma\left(1 - H, \frac{\pi}{4}n_m^2 s^2\right)\right]. \tag{3}$$

Here $m = l,u$ and $\Gamma(a, x)$ is the incomplete gamma function. In the limit as $n_l \to 0$ and $n_u \to \infty$, (1) reduces to the power variogram $\gamma(s) = C_0 s^{2H}$ with $C_0 = C\Gamma(1 - 2H)/2H$ for

exponential modes and $C_0 = C(\pi/4)^H \Gamma(1 - H)/2H$ for Gaussian modes, Γ being the gamma function. For $n_l \neq 0$ ($\lambda_l < \infty$, corresponding to a finite window), the variogram (1) defines a homogeneous field associated with a finite variance, $\sigma^2(n_l, n_u) = \sigma^2(n_l) - \sigma^2(n_u)$, where

$$\sigma^2(n_m) = \frac{C}{2Hn_m^{2H}}, \tag{4}$$

and a finite integral scale,

$$I(n_l, n_u) = \frac{2H}{1+2H} \frac{n_u^{1+2H} - n_l^{1+2H}}{n_u n_l \left(n_u^{2H} - n_l^{2H}\right)}. \tag{5}$$

2.2. Upscaled Permeability

[18] Consider three-dimensional steady state flow through a cube embedded in a multivariate Gaussian, statistically homogeneous and anisotropic log permeability field, $y = \ln k$, characterized by a truncated power variogram with $n_u = \infty$ ($\lambda_u = 0$), corresponding to zero support scale. Flow takes place under a uniform mean (across the ensemble of all y realizations) hydraulic gradient of magnitude J, acting between two constant head boundaries spaced a distance L apart. The other four boundaries are no-flow in the mean. Let $q(\mathbf{x})$ be the corresponding mean flux at any point $\mathbf{x}$ within the cube and define the effective permeability $k_{\text{eff}}(\mathbf{x})$ of the box at $\mathbf{x}$ via

$$q(\mathbf{x}) = \alpha k_{\text{eff}}(\mathbf{x}) J, \tag{6}$$

where α is the ratio between the unit weight and dynamic viscosity of the fluid. Upon invoking a conjecture owing to *Landau and Lifshitz* [1960], *Di Federico et al.* [1999] find that

$$\frac{k_{\text{eff}}(\mathbf{x})}{k_g} = \exp\left\{\sigma^2(\lambda_l)\left[\frac{1}{2} - D(\mathbf{x}, H, \mu)\right]\right\}, \tag{7}$$

where k_g is the geometric mean of k ($\ln k_g$ being the mean of y) and σ^2 (λ_l) is the variance of y, given by equation (4). The function D, given by equation (50) of Di Federico et al., depends on the correlation structure of y and on

$$\mu = \lambda_l / L. \tag{8}$$

Averaging equation (7) over the box yields k_{eq}/k_g where k_{eq} is the equivalent permeability of the box, independent of $\mathbf{x}$.

3. Interpretation of Observed Permeability Scale Effect

[19] We saw earlier that 1-m scale log permeability data from single-hole pneumatic injection tests at the ALRS fit an omnidirectional power variogram (Figure 3), representing a nonstationary random field with homogeneous spatial increments. We note in passing that the power variogram is characterized by $2H = 0.43$, which is close to the generalized value of $2H = 0.5$ deduced by one of us from an analysis of apparent dispersivities [*Neuman*, 1990] and permeabilities [*Neuman*, 1994] at many sites.

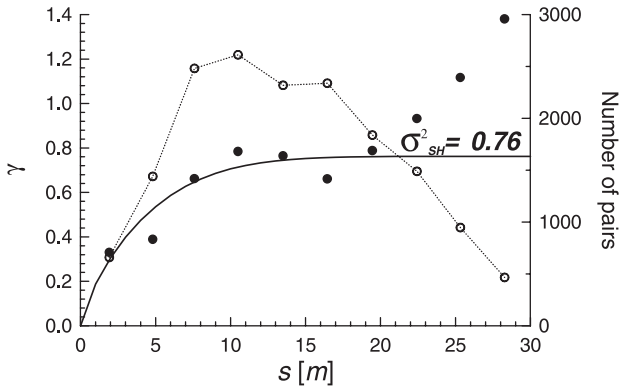

Figure 4. Truncated Gaussian variogram model (solid curve) with $C_0 = 0.19$, $2H = 0.75$, $\sigma^2_{SH} = 0.76$, and $\lambda_{l-SH} = 9.02$ m fitted to 1-m scale single-hole $\log_{10} k$ data (solid circles). Open circles represent number of data pairs.

3.1. Fitting a Truncated Power Variogram to 1-m Scale Single-Hole Test Data

[20] As the 1-m scale $\log_{10} k$ data represent a sample from a finite window, it is of interest to check how well they fit a truncated power variogram of type equations (1)–(3). Considering that the nominal support scale (1 m) is small relative to the window scale (a few tens of meters), we set the upper (high frequency) cutoff scale λ_u equal to zero (corresponding to $n_u = \infty$) in our analysis. We found that a truncated variogram consisting of Gaussian modes (equation (3)) fits the data much better than one consisting of exponential modes (equation (2)). In fitting a model to the sample variogram data (solid circles in Figure 4) we weighted them in relation to the number of $\log_{10} k$ pairs (open circles) on which they are based. The root-mean-square error of the fit was about the same for $2H = 0.75$ as for 1 but slightly higher for $2H = 0.5$. We therefore adopted a truncated variogram consisting of Gaussian modes with $C_0 = 0.19$, $2H = 0.75$, sill (variance) $\sigma^2_{SH} = 0.76$, lower cutoff scale $\lambda_{l-SH} = 9.02$ m, and integral scale $I = 3.87$ m to represent the 1-m scale single-hole permeability data in our analysis. This theoretical variogram is shown by a solid curve in Figure 4.

[21] Considering that permeabilities obtained from single-hole tests represent a small rock volume in the close vicinity of each test interval, we consider the rock volume associated with all of these tests to be that spanned by boreholes V2, W2a, X2, Y2, Y3, and Z2 in Figure 1. The smallest brick-shaped volume that embeds these boreholes measures $31 \times 20 \times 28$ m^3. We take the geometric mean dimension of this volume, $L_{SH} \approx 26$ m, to represent the nominal window scale of the single-hole test data. Then equation (8) implies that $\mu = \lambda_{l-SH}/L_{SH} \approx 0.35$. We note in passing that this is extremely close to the generalized value of $\mu \approx 1/3$ deduced by *Di Federico and Neuman* [1997] from an

analysis of apparent dispersivities [*Neuman*, 1990] and permeabilities [*Neuman*, 1994] at many sites.

3.2. Consistency With Equivalent and Tomographic $\log_{10}k$ Estimates From Cross-Hole Tests

[22] We now examine the extent to which the above truncated power variogram and corresponding parameters ($C_0 = 0.19$, $2H = 0.75$, $\sigma^2_{SH} = 0.76$, $\lambda_{l-SH} = 9.02$ m, $I_{SH} = 3.87$ m, and $\mu \approx 0.35$), obtained by direct geostatistical analysis of single-hole 1-m scale data $\log_{10}k$ data, are consistent with equivalent and tomographic $\log_{10}k$ estimates obtained by *Vesselinov et al.* [2001a, 2001b] through numerical inversion of cross-hole tests at the ALRS. Inverse interpretation of cross-hole tests was done by simulating airflow within a brick-shaped domain that measures $63 \times 54 \times 45$ m^3. We take the geometric mean dimension of this volume, $L_{CH} \approx 54$ m, to represent the nominal window scale of both the equivalent and tomographic $\log_{10}k$ estimates obtained by numerical inversion of the cross-hole tests. Since L_{CH} is twice as large as L_{SH}, a standard (as opposed to truncated) power variogram was used to generate the tomographic estimates. Figure 5 shows that overall, the inverse model fit had improved rapidly as $2H$ increased from 0.5 to 0.75 and more slowly or not at all as $2H$ increased beyond 0.75. This is consistent with behavior observed during our fit of a truncated power variogram to 1-m scale single-hole test data over a smaller window of scale L_{SH}. We therefore take $2H = 0.75$ to represent $\log_{10}k$ in our analysis of both the cross-hole and single-hole tests at the ALRS.

[23] We now ask how well does k_{eq}/k_g, the spatial average of equation (7), explain the apparent increase in log permeability when one compares the average values of single-hole and equivalent inverse estimates? For k_{eq}/k_g to explain this increase, equation (7) must be compatible with the truncated power variogram fitted earlier to the single-hole $\log_{10}k$ data. To what extent is it?

[24] The single-hole data have yielded $\mu \approx 0.35$. As the equivalent inverse estimates are associated with a window scale $L_{CH} \approx 54$ m, compatibility with the single-hole data implies that these estimates are associated with a lower cutoff scale of $\lambda_{l-CH} = \mu L_{CH} \approx 18.9$ m. This corresponds to an integral scale $I_{CH} \approx 8.10$ m.

[25] We take the logarithm of equivalent permeability, $\log_{10}k_{eq-CH}$, to be the spatial average of $\log_{10}k_{\text{eff}}(\mathbf{x})$ over the cube. Then equation (7) yields

$$\frac{k_{eq-CH}}{k_{g-CH}} = \exp\left\{2.303^2\sigma^2_{CH}\left[\frac{1}{2} - \bar{D}(H,\mu)\right]\right\}, \qquad (9)$$

where σ^2_{CH} is the variance of $\log_{10}k$ over a window of scale L_{CH} and $\bar{D}$ is the average value of D over the window. To avoid excessive computation, our results below are based on numerical averaging of D along three orthogonal lines parallel to the sides of the window that intersect at its center.

[26] In equation (9) we set k_{eq-CH} equal to the geometric mean of equivalent permeability estimates obtained by numerical inversion of one or more cross-hole tests while treating the rock as being spatially uniform. Strictly speaking, this would be valid only if airflow during each cross-hole test was uniform in the mean. In reality, airflow during each test diverges from a packed-off borehole injection interval in all directions. However, the three-dimensional effect of divergence on effective permeability dissipates entirely within about two integral scales from the injection interval, and nearly so within about one integral scale [*Indelman*, 2001, Figure 1]. Most distances between injection and monitoring intervals at the ALRS either exceed or are of the order of one integral scale, $I_{CH} = 8.10$ m [*Illman et al.*, 1998, Table 5.3]. We can therefore safely disregard the effect of flow divergence on our analysis.

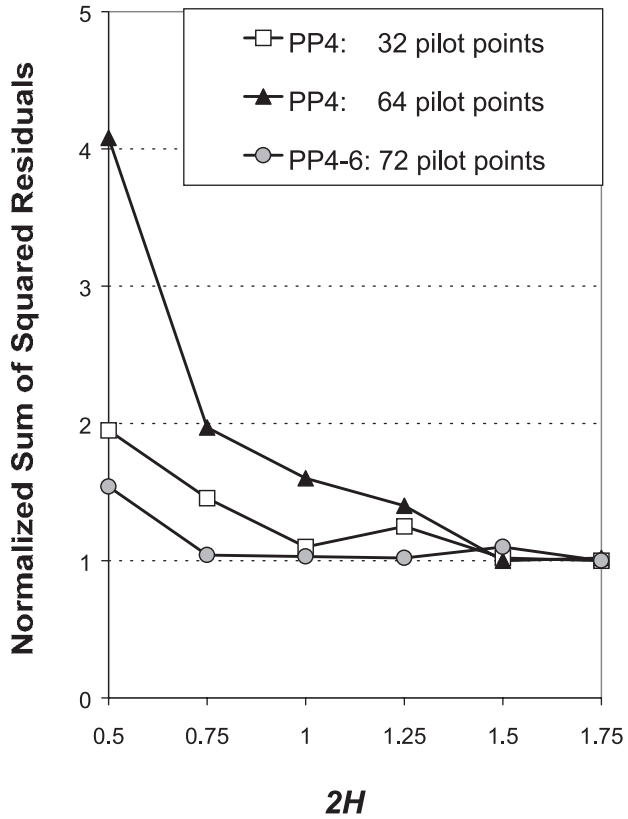

Figure 5. Sum of squared pressure residuals versus $2H$ for tomographic inversions of various cross-hole tests, normalized by smallest value (modified after *Vesselinov et al.* [2001b]).

[27] We set k_{g-CH} in equation (9) equal to the geometric mean of tomographic $\log_{10}k$ estimates obtained from the same cross-hole tests as those used to calculate k_{eq-CH}. Resulting values of σ^2_{CH} for three sets of cross-hole inverse estimates are listed in Table 2. Also listed in Table 2 are corresponding values of k_{eq-CH}, k_{g-CH}, k_{eq-CH}/k_{g-CH}, the variance σ^2_{CH-T} of tomographic inverse estimates, and $\sigma^2_{CH}/\lambda^{2H}_{l-CH}$.

[28] Two of the three estimates of σ^2_{CH} in Table 2, obtained from the upscaling formula (9), exceed the variance σ^2_{CH-T} of corresponding tomographic inverse estimates. Since the inverse estimates are smooth and cover a somewhat smaller volume than the simulation domain, their variance is indeed expected to be somewhat smaller than that of the underlying random field, σ^2_{CH}.

[29] Compatibility with equation (4) requires that the variance and cutoff scale of the random $\log_{10}k$ fields,

Table 2. Statistics of $\mathrm{Log}_{10}k$ Estimates From Cross-Hole Tests[a]

	$\log_{10}k_{eq-CH}$	$\log_{10}k_{g-CH}$	k_{eq-CH}/k_{g-CH}	σ^2_{CH}	σ^2_{CH-T}	$\sigma^2_{CH}/\lambda^{2H}_{l-CH}$
PP4: 32 pilot points	−13.57	−15.23	5.7	2.05	1.67	0.23
PP4: 64 pilot points	−13.57	−14.77	15.8	1.48	1.62	0.16
PP4–PP6: 72 pilot points	−13.70	−15.69	97.7	2.46	1.93	0.27

[a] $\mathrm{Log}_{10}k$ values are m^2.

which underlie the single- and cross-hole test results, scale according to

$$\frac{\sigma^2_{SH}}{\lambda^{2H}_{l-SH}} = \frac{\sigma^2_{CH}}{\lambda^{2H}_{l-CH}}. \quad (10)$$

In fact, this relationship is satisfied almost exactly in the case of inverse estimates obtained with the aid of 64 pilot points from cross-hole test PP4, where $\sigma^2_{CH}/\lambda^{2H}_{l-CH} = 0.16$ (Table 2) in comparison to $\sigma^2_{SH}/\lambda^{2H}_{l-SH} \approx 0.15$. These estimates were ranked by four model discrimination criteria as being the best among those considered in Table 2 [*Vesselinov et al.*, 2001b].

[30] Estimates based on test PP4 with 32 pilot points were ranked second best among the three in Table 2, and those based on the simultaneous interpretation of tests PP4, PP5, and PP6 with 72 pilot points were ranked last [*Vesselinov et al.*, 2001b]. This reduced quality of the latter two inverse estimates may help explain why the first among them yields $\sigma^2_{CH}/\lambda^{2H}_{l-CH} \approx 0.23$ and the second yields $\sigma^2_{CH}/\lambda^{2H}_{l-CH} \approx 0.27$, exceeding $\sigma^2_{SH}/\lambda^{2H}_{l-CH}$ by factors of 1.5 and 1.8, respectively. Another explanation may be related to uncertainty in our estimate of the window scales L_{l-SH} and L_{l-CH}, both of which affect the value of μ, which impacts directly on our calculations.

[31] Figure 6 shows how the normalized equivalent pneumatic permeability, k_{eq}/k_g, corresponding to each of the three estimates in Table 2, scale up and down with domain size L, according to equation (9) (circles represent the k_{eq-CH}/k_{g-CH} values in Tables 2). The spread between these curves is a reflection of uncertainty in our ability to quantify and interpret the observed scale effect at the ALRS.

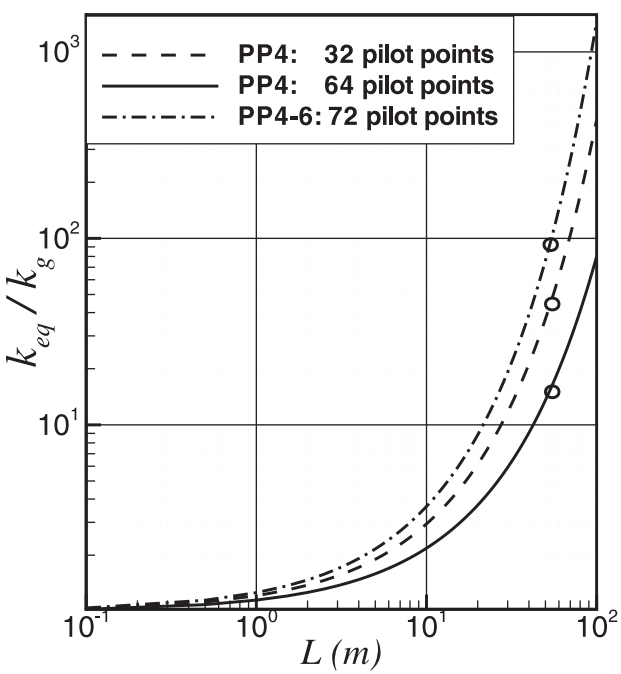

Figure 6. Normalized equivalent pneumatic permeability of unsaturated fractured tuff at Apache Leap Research Site (ALRS), k_{eq}/k_g, versus domain scale L for the three sets of cross-hole inverse results in Table 2.

4. Conclusions

1. There is a very pronounced scale effect in air permeability at the ALRS. As there is consistency between single-hole and cross-hole test results, the scale effect is unrelated to the method of testing. As there is consistency between results obtained by means of diverse steady state and transient, analytical and numerical methods of test interpretation, the scale effect is unrelated to the method of interpretation. As neither the single-hole nor the cross-hole test results have been affected by any skin effect of consequence, the scale effect is unrelated to phenomena associated with borehole drilling and completion. The observed permeability scale effect at the ALRS appears to be real.

2. We have asked ourselves to what extent can one interpret the observed permeability scale effect at the ALRS by means of a stochastic scaling theory of *Di Federico and Neuman* [1997] and *Di Federico et al.* [1999], which views log permeability as a truncated random fractal. There is considerable uncertainty about the magnitude of the observed scale effect at the ALRS, making it difficult for us to answer this question conclusively. However, there is sufficient correspondence between the site data and the theory to suggest that the latter may indeed provide a viable (if not complete) explanation of the observed scale effect.

[32] **Acknowledgments.** This research was supported in part by the U.S. Nuclear Regulatory Commission under contracts NRC-04-95-038 and NRC-04-97-056. Additional support was provided by the Italian Ministero dell'Università e della Ricerca Scientifica e Tecnologica (MURST) 40% "Metodologie innovative per il monitoraggio, la gestione ed il controllo quali-quantitativo delle acque sotterranee."

References

Bradbury, K. R., and M. A. Muldoon, Hydraulic conductivity determinations in unlithified glacial and fluvial materials, in *Ground Water and Vadose Zone Monitoring*, edited by D. M. Nielson and A. I. Johnson, *ASTM Spec. Tech. Publ.*, *1053*, 138–151, 1990.

Butler, J. J., Jr., and J. M. Healey, Relationship between pumping-test and slug-test parameters: Scale effect or artifact?, *Ground Water*, *36*(2), 305–313, 1998a.

Butler, J. J., Jr., and J. M. Healey, Discussion of papers: Authors' reply, *Ground Water*, *36*(6), 867–868, 1998b.

Chen, G., W. A. Illman, D. L. Thompson, V. V. Vesselinov, and S. P. Neuman, Geostatistical, type curve and inverse analyses of pneumatic injection tests in unsaturated fractured tuffs at the Apache Leap Research Site near Superior, Arizona, in *Dynamics of Fluids in Fractured Rocks*, *Geophys. Monogr. Ser.*, vol. 122, edited by B. Faybishenko, et al., pp. 73–98, AGU, Washington, D. C., 2000.

Di Federico, V., and S. P. Neuman, Scaling of random fields by means of truncated power variograms and associated spectra, *Water Resour. Res.*, *33*(5), 1075–1085, 1997.

Di Federico, V., S. P. Neuman, and D. M. Tartakovsky, Anisotropy, lacunarity, upscaled conductivity and its covariance in multiscale fields with truncated power variograms, *Water Resour. Res.*, *35*(10), 2891–2908, 1999.

Geldon, A. L., Results and interpretation of preliminary aquifer tests in boreholes UE-25c #1, E-25c #2, and UE-25c #3, Yucca Mountain, Nye County, Nevada, *U.S. Geol. Surv. Water Resour. Invest. Rep.*, *94-4177*, 119 pp., 1996.

Guzman, A., S. P. Neuman, C. Lohrstorfer, and R. Bassett, Chapter 4, in *Validation Studies for Assessing Flow and Transport Through Unsaturated Fractured Rocks*, edited by R. Bassett, et al., *NUREG/CR-6203*, U.S. Nucl. Regulatory Comm., Washington, D. C., Aug. 1994.

Guzman, A. G., A. M. Geddis, M. J. Henrich, C. F. Lohrstorfer, and S. P. Neuman, Summary of air permeability data from single-hole injection tests in unsaturated fractured tuffs at the Apache Leap Research Site: Results of steady-state test interpretation, *NUREG/CR-6360*, U.S. Nucl. Regulatory Comm., Washington, D. C., 1996.

Illman, W. A., and S. P. Neuman, Type-curve interpretation of multi-rate single-hole pneumatic injection tests in unsaturated fractured rock, *Ground Water*, *38*(6), 899–911, 2000.

Illman, W. A., and S. P. Neuman, Type-curve interpretation of a cross-hole pneumatic injection test in unsaturated fractured tuff, *Water Resour. Res.*, *37*(3), 583–603, 2001.

Illman, W. A., D. L. Thompson, V. V. Vesselinov, and S. P. Neuman, Single-hole and cross-hole pneumatic tests in unsaturated fractured tuffs at the Apache Leap Research Site: Phenomenology, spatial variability, connectivity and scale, *Rep. NUREG/CR-5559*, U. S. Nucl. Regulatory Comm., Washington, D. C., Sept. 1998.

Indelman, P., Steady-state source flow in heterogeneous porous media, *Transp. Porous Media*, *45*(1), 105–127, 2001.

Landau, L. D., and E. M. Lifshitz, *Electrodynamics of Continuous Media*, Pergamon, New York, 1960.

Martínez-Landa,, L., J. Carrera, J. Guimerá, E. Vazquez-Suñé, L. Vives, and P. Meier, Methodology for the hydraulic characterization of a granitic block, in *Calibration and Reliability in Groundwater Modelling; Coping with Uncertainty, ModelCARE 99*, edited by F. Stauffer, et al., *IAHS Publ.*, *265*, 340–345, 2000.

Neuman, S. P., Universal scaling of hydraulic conductivities and dispersivities in geologic media, *Water Resour. Res.*, *26*(8), 1749–1758, 1990.

Neuman, S. P., Generalized scaling of permeabilities: Validation and effect of support scale, *Geophys. Res. Lett.*, *21*(5), 349–352, 1994.

Rasmussen, T. C., D. D. Evans, P. J. Sheets, and J. H. Blanford, Unsaturated fractured rock characterization methods and data sets at the apache leap tuff site, *NUREG/CR-5596*, U.S. Nucl. Regulatory Comm., Washington, D. C., 1990.

Rasmussen, T. C., D. D. Evans, P. J. Sheets, and J. H. Blanford, Permeability of Apache Leap Tuff: Borehole and core measurements using water and air, *Water Resour. Res.*, *29*(7), 1997–2006, 1993.

Rasmussen, T. C., S. C. Rhodes, A. Guzman, and S. P. Neuman, Apache Leap Tuff INTRAVAL experiments: Results and lessons learned, *NUREG/CR-6096*, U.S. Nucl. Regulatory Comm., Washington, D. C., 1996.

Rovey, C. W., II, Digital simulation of the scale effect in hydraulic conductivity, *J. Hydrol.*, *6*, 216–225, 1998.

Rovey, C. W., II, and D. S. Cherkauer, Scale dependency of hydraulic conductivity measurements, *Ground Water*, *33*, 769–780, 1995.

Rovey, C. W., II, and W. L. Niemann, Wellskins and slug tests: Where's the bias?, *J. Hydrol.*, *243*, 120–132, 2001.

Sánchez-Villa, X., J. Carrera, and J. P. Girardi, Scale effects in transmissivity, *J. Hydrol.*, *183*, 1–22, 1996.

Schertzer, D., and S. Lovejoy, Nonlinear variability in geophysics: Multifractal simulations and analysis, in *Fractals: Physical Properties and Origin*, edited by L. Pietronero, pp. 4–79, Plenum, New York, 1989.

Schmitt, F., S. Lovejoy, and D. Schertzer, Multifractal analysis of the Greenland Ice Core Project climate data, *Geophys. Res. Lett.*, *22*, 1689–1692, 1995.

Schulze-Makuch, D., D. A. Carlson, D. S. Cherkauer, and P. Malik, Scale dependency of hydraulic conductivity in heterogeneous media, *Ground Water*, *37*, 904–919, 1999.

Tidwell, V. C., and J. L. Wilson, Laboratory method for investigating permeability upscaling, *Water Resour. Res.*, *33*(7), 1607–1616, 1997.

Vesselinov, V. V., and S. P. Neuman, Numerical inverse interpretation of single-hole pneumatic tests in unsaturated fractured tuff, *Ground Water*, *39*(5), 685–695, 2001.

Vesselinov, V. V., S. P. Neuman, and W. A. Illman, Three-dimensional numerical inversion of pneumatic cross-hole tests in unsaturated fractured tuff, 1, Methodology and borehole effects, *Water Resour. Res.*, *37*(12), 3001–3017, 2001a.

Vesselinov, V. V., S. P. Neuman, and W. A. Illman, Three-dimensional numerical inversion of pneumatic cross-hole tests in unsaturated fractured tuff, 2, Equivalent parameters, high-resolution stochastic imaging and scale effects, *Water Resour. Res.*, *37*(12), 3019–3041, 2001b.

Y. Hyun and S. P. Neuman, Department of Hydrology and Water Resources, University of Arizona, Tucson, Arizona 85721, USA.

V. V. Vesselinov and D. M. Tartakovsky, Los Alamos National Laboratory, Los Alamos, New Mexico 87545, USA.

W. A. Illman, University of Iowa, Iowa City, IA 52242, USA.

V. Di Federico, University of Bologna, Bologna, Italy.